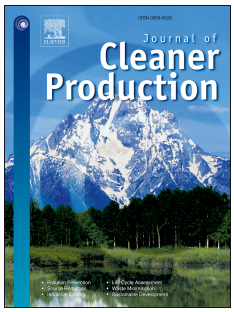
Journal Pre-proof



Cooperative control strategy for plug-in hybrid electric vehicles based on a hierarchical framework with fast calculation

Yuanjian Zhang, Chong Guo, Guang Li, Yonggang Liu, Zheng Chen

PII: S0959-6526(19)34497-X

DOI: https://doi.org/10.1016/j.jclepro.2019.119627

Reference: JCLP 119627

To appear in: *Journal of Cleaner Production*

Received Date: 22 August 2019

Revised Date: 15 November 2019

Accepted Date: 8 December 2019

Please cite this article as: Zhang Y, Guo C, Li G, Liu Y, Chen Z, Cooperative control strategy for plug-in hybrid electric vehicles based on a hierarchical framework with fast calculation, *Journal of Cleaner Production* (2020), doi: https://doi.org/10.1016/j.jclepro.2019.119627.

This is a PDF file of an article that has undergone enhancements after acceptance, such as the addition of a cover page and metadata, and formatting for readability, but it is not yet the definitive version of record. This version will undergo additional copyediting, typesetting and review before it is published in its final form, but we are providing this version to give early visibility of the article. Please note that, during the production process, errors may be discovered which could affect the content, and all legal disclaimers that apply to the journal pertain.

© 2019 Published by Elsevier Ltd.

Journal Pre-proof

Cooperative Control Strategy for Plug-in Hybrid Electric Vehicles Based on a Hierarchical Framework with Fast Calculation

Yuanjian Zhang[1], Chong Guo[1], Guang Li[2], Yonggang Liu[3*], Zheng Chen[4*]
[1] State Key Laboratory of Automotive Dynamic Simulation and Control, College of Automotive Engineering, Jilin University, Changchun, 130022, China
[2] School of Engineering and Materials Science, Queen Mary University of London, London, E1 4NS, UK
[3] State Key Laboratory of Mechanical Transmission & School of Automotive Engineering, Chongqing University, Chongqing, 400044, China
[4] Faculty of Transportation Engineering, Kunming University of Science and Technology, Kunming, 650500, China
Corresponding Authors: Zheng Chen (chen@kust.edu.cn) and Yonggang Liu (andylyg@umich.edu)

Abstract: Developing optimal control strategies with capability of real-time implementation for plug-in hybrid electric vehicles (PHEVs) has drawn explosive attention. In this study, a novel hierarchical control framework is proposed for PHEVs to achieve the instantaneous vehicle-environment cooperative control. The mobile edge computation units (MECUs) and the on-board vehicle control units (VCUs) are included as the distributed controllers, which enable vehicle-environment cooperative control and reduce the computation intensity on the vehicle by transferring partial work from VCUs to MECUs. On this basis, a novel cooperative control strategy is designed to successively achieve the energy management planned by the iterative dynamic programming (IDP) in MECUs and the energy utilization management achieved by the model predictive control (MPC) algorithm in the VCU. The performance of raised control strategy is validated by simulation analysis, highlighting that the cooperative control strategy can achieve superior performance in real-time application that is close to the global optimization results solved offline.

Key words: Cooperative control strategy, hierarchical framework, iterative dynamic programming (IDP), model predictive control (MPC), plug-in hybrid electric vehicles (PHEVs)

NOMENCLATURE

Abbreviations

PHEVs	plug-in hybrid electric vehicles	MPC	model predictive control
MECUs	mobile edge computation units	EDA	estimation of distribution algorithm
VCUs	vehicle control units	ACC	adaptive cruise controller

Journal Pre-proof

IDP	iterative dynamic programming	QP	quadratic programming
MPC	model predictive control	CPSs	cyber-physical systems
GHG	greenhouse gas	MEC	mobile-edge computation
ICE	internal combustion engine	IDP	iterative dynamic programming
EMSs	energy management strategies	CGS	cloud global server
DP	dynamic programming	IoV	internet of vehicle
PMP	Pontryagin's minimum principle	BS	base station
QP	quadratic programming	CCA	cooperative collision avoidance
ECMS	equivalent minimization consumption strategy	DSRC	short range communication
A-ECMS	adaptive equivalent minimization consumption strategy	GPS	global position system
SDP	stochastic dynamic programming	HDA	hybrid driving assist
NNs	neural networks	HDC	hybrid driving charge
ITSs	intelligent transportation systems	PMSM	permanent magnet synchronous motor
ODE	ordinary differential equation	BSFC	brake-special fuel consumption

Symbols

P_{req}	required tractive power	E_{e_target}	target electric energy consumption
G	gravity	$x_{k_\max}^{q+1}$	upper boundary of state variables at step k in iteration $q+1$
a	gradient	$x_{k_min}^{q+1}$	lower boundary of state variables at step k in iteration $q+1$
f	rolling resistance factor	$x_{k_{opt}}^{q}$	optimal state variable at step k in iteration q
C_D	aerodynamic drag factor	$u_{k_{opt}}^{q}$	optimal control variable at step k in iteration q
A	frontal area	$u_{k_\max}^{q}$	upper boundary of control variables at step k in iteration q
v	aerodynamic drag factor	$u_{k_min}^{q}$	lower boundary of control variables at step k in iteration q
ξ	correction coefficient of rotating mass	α	contracted ratio
η_t	transmission efficiency	β	contracted ratio
m	vehicle mass	v_{ave}	average speed in certain route segment
T_{req}	required tractive torque	v_{std}	velocity standard deviation in certain route segment

Journal Pre-proof

T_{fuel_path}	tractive torque provided by the fuel path	E_{e_basic}	estimated electric energy consumption
T_{ele_path}	tractive torque provided by the electric path	$P_{eng_{opt}}$	engine power corresponding to the optimal operation points
T_{eng}	engine torque	T_f	traffic factor
T_{em}	electric motor torque	x	state inputs
i_{gb}	gear ratio	u	control inputs
i_{fd}	final drive ratio	s	distance step
n_g	gear number	s_f	terminal state
R_{wh}	wheel radius	y	control output
η_{eng}	engine net efficiency	Q	penalty matrixes in MPC based optimal tracking
ω_{eng}	rotating speed of engine	R	penalty matrixes in MPC based optimal tracking
Q_{lhv}	fuel lower heating value	n_p	prediction length
$\dot{m}_f$	fuel consumption rate	A_e	parameter matrixes in ODE
ω_{em}	angular speed of electric motor	B_e	parameter matrixes in ODE
P_{em}	power of electric motor	C_e	parameter matrixes in ODE
η_{mot}	motor efficiency in tractive mode	Θ	resulting matrix in QP solving
η_{gen}	m efficiency in generator mode	Θ	resulting matrix in QP solving
SOC	state of charge	Ψ	resulting matrix in QP solving
V_{oc}	open circuit voltage of battery	Q_1	penalty matrixes in MPC based optimal tracking
R_{int}	internal resistance of battery	Q_2	penalty matrixes in MPC based optimal tracking
P_{batt}	battery power	R	penalty matrixes in MPC based optimal tracking
Δs	battery capacity	W	constant matrix in MPC based optimal tracking
x_k^i	ith state variable at step k	M_1	constant matrix in MPC based optimal tracking
u_k^j	ith control variable at step k	M_2	constant matrix in MPC based optimal tracking
h_k	stage cost	$\aleph$	prediction set
F_k	state function	g	gravity acceleration
ω_t	weight on electric energy consumption	Δs	calculation step
E_{e_real}	real electric energy consumption	k	simulation in MPC algorithm

Journal Pre-proof

Journal Pre-proof

I. INTRODUCTION

Nowadays, greenhouse gas (GHG) emissions, environmental pollution and irreversible natural resource shortage are representative adverse effects from automobile industry on society, and spark desperate demand on effective solutions to relieve the severe problems. Researchers from industry and academia have conquered a variety of effective solutions, including plug-in hybrid electric vehicles (PHEVs) [1, 2]. PHEVs, usually equipped with a high efficient internal combustion engine (ICE) and a large capacity battery pack, can provide more efficient driving performance with higher fuel economy as well as less GHG and harmful exhaust emissions [3]. By means of proper power allocation schemes supplied by energy management strategies (EMSs), the ICE and battery can operate co-ordinately and efficiently under different driving conditions. Proper design of EMSs is critical to fully excavate performance potential of PHEVs. The powertrain of PHEVs, however, is a highly nonlinear and complex system [4], rendering it a challenging task to investigate effective EMSs with optimal performance and capability in real-time implementation.

Recently, a great number of EMSs have been spurred which can be mainly divided into three categories, i.e., rule-based strategies, global optimization-based strategies and instantaneous optimization-based strategies. The conventional rule-based strategies, such as threshold value strategies [5] and fuzzy logic strategies [6], are widely accepted by industry because of its simplicity, high efficiency and easy application in engineering practice. However, they are far from optimal as most of them is developed by relying only on expert knowledge. To improve overall performance of rule-based methods, optimization algorithms are introduced to optimize the threshold values together with the included rules [7, 8]. This kind of optimization, nevertheless, is conducted based on only certain or several driving cycles, resulting in poor adaptability to diverse driving conditions. The global optimization-based algorithms [9], including dynamic programming (DP) [10], Pontryagin's minimum principle (PMP) [2] and quadratic programming (QP) [11], can find optimal solutions in the whole given driving cycle and finally formulate the optimal control policy for each step from the perspective of global optimization. Owning to the special manners of searching optimal solutions, global optimization-based methods cannot be effectively applied without knowing the future driving conditions in advance [12-14]. In addition, high computation intensity also prevents them from online

Journal Pre-proof

application. The instantaneous optimization-based EMSs have been validated to behave reasonably with the closer performance, compared with global optimization-based EMSs [15, 16]. Popular candidates, including equivalent minimization consumption strategy (ECMS) [17], and model predictive control (MPC) algorithms [18], have shown great potential in real-time application. Despite the competent performance in real application, the instantaneous algorithms are also widely affected by the driving cycle information, e.g., the equivalent factor of ECMS needs to adjusted dynamically [19-21], thus discounting application performance in real-time implementation.

The present methods seem to be constrained by different issues when applied online. To overcome them, investigators have also gained remarkable progresses by fully incorporating the environmental information [22]. To relieve tight dependence on driving cycle information, some augmented methods such as adaptive EMCSs (A-ECMSs) [16] and stochastic DP (SDP) [23], are proposed when subject to different conditions and constraints. The improved methods mainly focus on identifying and predicting driving conditions online [24, 25]. By merging road style identification and velocity prediction into EMSs, the real-time controlling performance can be further improved [26]. With the help of identified road styles and forecasted velocity profiles, specific inner parameters can be assigned the algorithms, thus enabling adaptive control. It is admitted that the modified EMSs show great merits, whereas methods of classifying the road conditions, like neural networks (NNs) [27], and of predicting the velocity profiles, such as Markov Chain [28], impose huge pressure on on-board calculation resources. In addition, it is intractable to predict the velocity profile accurately, as the future driving behaviours are determined not only by drivers, but also by environment factors [29]. As such, the vehicle-environment cooperative control is particularly encouraged to integrate more environmental information into the vehicle control.

With the development of intelligent transportation systems (ITSs), communication technologies and cyber-physical systems (CPSs), the vehicle-environment cooperative control has attracted wide attention and has been developed substantially [30]. Road traffic information shared by volunteer vehicles can be easy accessed by the target vehicle, and thus supplies potential valuable inputs for cooperative energy management. Consequently, multi-level strategies are spurred trying to calculate optimal control policies offline firstly in the high-level layer based on the global optimization

Journal Pre-proof

methods according to the shared traffic information, and then the optimal control results are implemented in the low-level layer as the global reference for immediate control [31, 32]. The strategy in the low-level controller is requested to accomplish instantaneous energy management with the help of global optimal policies [31, 32]. The raised cooperative hierarchical control strategies are laudable except that the offline calculation before the trip commencement still costs much time, and leads to huge computation burden on the vehicle hardware.

Commercialization of the fifth-generation communication technologies and emergence of mobile-edge computation (MEC) provide a new solution media to optimize the cooperative control strategies for PHEVs [33, 34]. By implementing MEC, some computation, originally completed in on-board VCUs, can be transferred to the computation sources at route side [35]. The shared traffic information can also be collected and completely processed by the MEC units. Even though the cooperative control strategies in previous research have shown satisfactory capabilities to improve fuel economy of PHEVs in practice, tricky shortcomings still remain in accelerating computation speed without sacrificing optimal control effect. For the cooperative control strategies based on hierarchical architectures, the narrowed optimization range in the top level when planning the optimal trajectory of variable (usually battery state of charge (SOC)) indeed lessens the calculation intensity, and the offline optimization results might by deteriorated as it may not be the global optimization in the whole trip. Therefore, it is rather worthy to further investigate cooperative control strategies with advanced architecture that extraordinarily balance computation burden and controlling effect.

Motivated by this, a novel cooperative EMS for PHEVs is herein proposed based on a hierarchical framework with reasonable capability in real-time application. The exclusive hierarchical controlling framework, consisting of MECUs and on-board VCUs, is fully qualified for the vehicle-environment control. In MECUs that belong to different route segments, the optimal battery SOC trajectory is quantitatively planned by the iterative DP (IDP) according to the collected traffic information; and subsequently in on-board VCUs, the MPC is employed to resolve the final energy management by tracking the designed reference SOC trajectory. Unlike the battery SOC trajectory planning methods in literature [10], the raised EMS employs IDP to plan the optimal battery SOC trajectory in each route segment instead of the whole trip, thereby effectively alleviating computation

Journal Pre-proof

burden. By benefiting from the adaptive object function in IDP, the battery SOC trajectory can be quantitatively programmed based on permitted energy consumption that is derived from the shared traffic information. Numerical simulation is conducted to validate the performance of proposed strategy. The effectiveness of raised method is comparatively studied in diverse driving conditions. The main contributions of this study are attributed to the following two main aspects:

1) A service-oriented hierarchical framework is built to uphold the vehicle-environment cooperative control. The MECUs participate in global optimization to lessen the computation intensity that originally imposes on the on-board VCUs, thereby accelerating the calculation speed in real-time implementation. By taking advantage of the superior calculation ability of MEC in cooperative control and management, the personalized information from vehicles on routes can be easier to be collected and incorporated into development of EMS.

2) A cooperative control strategy is proposed based on the hierarchical framework. The control action is executed through a two-stage process. In the first stage (energy utilization plan), the optimal battery SOC trajectories in each divided route segment are rapidly planned by the IDP in MECUs according to the allowed electric energy consumption extracted from the shared traffic information data. The narrowed optimization scope from the whole trip into route segments enables reduction of the computation labour, and simultaneously the application of IDP with quantitative adjustment on electric energy consumption shrinks the difference from that by deterministic DP in the whole trip. In the second stage (energy utilization management), the MPC achieves the immediate energy management in on-board VCUs by tracking the reference trajectories.

The remained of this paper is organized as follows. The hierarchical framework and vehicle model are introduced in Section II. Section III elaborates the newly developed cooperative control strategy. Section IV discusses the simulation results and comparatively validates the performance of raised strategy, followed by the main conclusions drawn in Section V.

II. Foundation of the Strategy: Hierarchical Framework and Vehicle Model

2.1 Hierarchical Framework for the Cooperative Control Strategy

The newly designed hierarchical framework, illustrated in Fig. 1, is a publish-subscribe paradigm for vehicle-environment cooperative control. In it, there are three kinds of synergistic controllers:

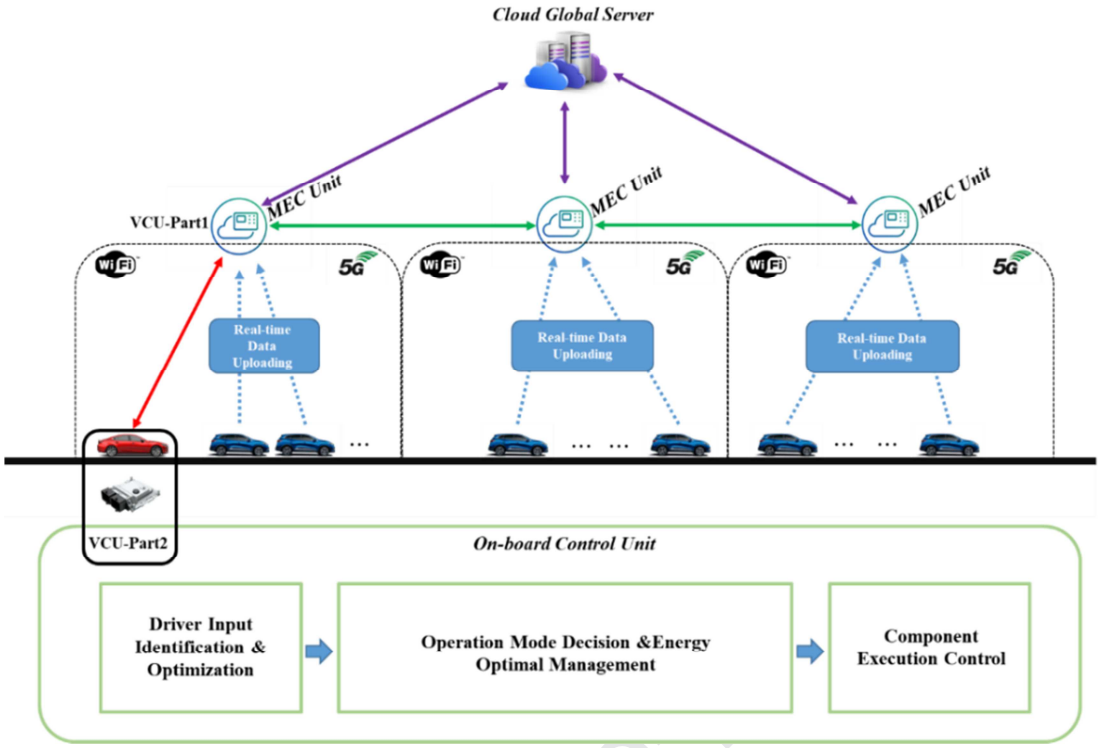


Fig. 1. The hierarchical framework for the vehicle-environment cooperative control.

Cloud Global Server (CGS):

CGS is the central processing unit that coordinates and monitors computation sources according to the control request sent from vehicles via the relay of MECUs. To be specific, CGS will pick up the corresponding MECUs to participate in the controlling process according to vehicle control request and travel route. CGS will also monitor the controlling process in MECUs and govern their communication mutually for sharing valuable information.

Mobile Edge Computation Unit (MECU):

MECUs, normally deployed at roadside, share the computation burden originally imposed on vehicle on-board controllers and CGS. The working scope of each MECU will be constrained within a short route segment, assuring that the calculated amount will not surpass the hardware capability in the MECU. The shared traffic information from volunteer vehicles on the certain route segment, including the vehicle global position system (GPS) coordinates, vehicle velocities, distances to front vehicles, and travel destinations, will be sent to MECUs. They can process the whole information to generate some intermediate variables, such as velocity profiles for future driving, and complete certain control process accordingly under the command from CGS.

On-Board Vehicle Control Unit (VCU):

VCU is the mobile controlling unit under the cooperative control framework, in which the control processes are implemented to accomplish final control for the vehicle. In particular, VCU will generate the control order to main powertrain components in terms of driving request and environmental information. In the cooperative control system, VCU will also send the synergistic control requirement to MECUs and CGS. We consider a MEC-based internet of vehicle (IoV) system, as shown in Fig. 2, where the MECU is mounted at the base station (BS) and owns enough computational capability. Moreover, we suppose the cooperative collision avoidance (CCA) [36] communication protocol is adopted, which is an emerging vehicular safety application using the IEEE- and ASTM-adopted dedicated short range communication (DSRC) standard. The vehicle is equipped with a single antenna. On this basis, the MEC-based time frame is described in Fig. 3. For the channel estimation, the vehicle needs to transmit a small number of pilot signals to BS, and then BS estimates the channel. Subsequently, the vehicle offloads the input data to BS, and the MEC server performs calculation. Finally, BS sends back the computing results (controlling information) to the vehicle. Since the transmitted data both at the channel estimation and return control information phases are quite small, the transmission time is extremely short and thus can be ignored.

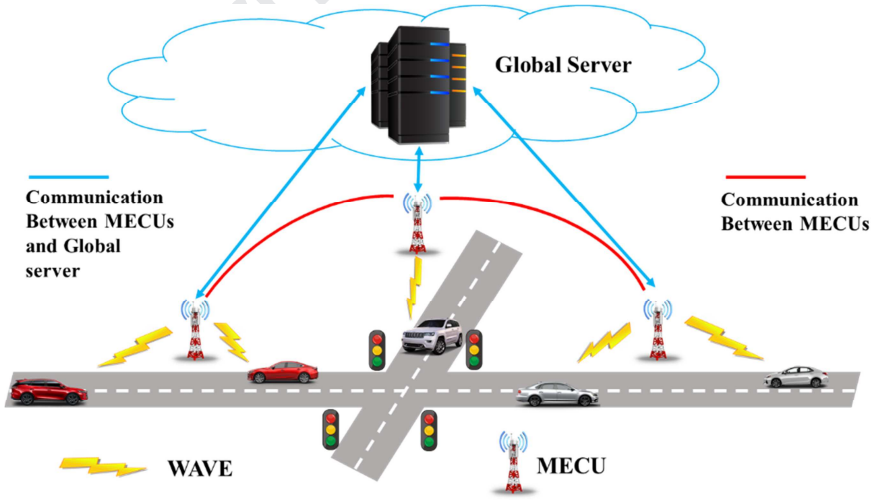


Fig. 2. MEC-based IoV system.

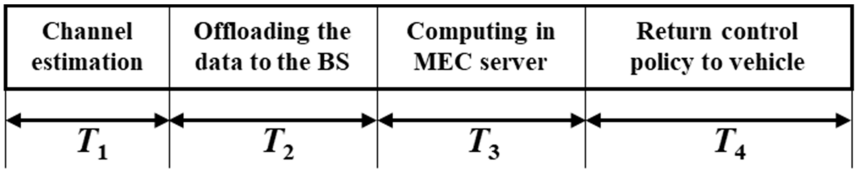


Fig. 3. The time frame for the MEC-based IoV.

Journal Pre-proof

Based on the developed hierarchical framework, essentially, the concept of VCU is extended in this study. The originally integrated VCU is reshaped into a multi-class controller with one part in a vehicle and the other part in cloud. The computation burden of each part in the reshaped controller is alleviated, thus providing a certain room to design more efficient cooperative control strategies for real-time implementation. After fully considering the communication speed, bandwidth, reliability and cost, the MECU is assumed to be installed with an average distance of 1.5 km between two segments [34]. The presented hierarchical framework, actually, is an architecture with high expansibility, and is also competitive to support the multi-vehicle energy collaborative optimization. In this paper, we mainly focused on the performance improvement of energy management in single vehicle by the novel hierarchical framework, trying to validate the corresponding algorithms and fundamental mechanism first and preparing for future study on multi-vehicle collaborative management.

2.2 Configuration and Model of the Studied Parallel PHEV

2.2.1 Configuration of the Studied Parallel PHEV

A single axle parallel PHEV is studied to investigate the cooperative control strategy. The configuration of the selected PHEV is depicted in Fig. 4. In the fuel path, a 2.0-Litre Atkinson ICE provides the tractive force. In the electric path, a 124 kW electric motor is responsible for supplying the tractive torque and recycling the braking energy. The recycled braking energy will be stored in a 6.7 kWh lithium-ion battery pack. The tractive torque from ICE plus the electric torque from motor will be transmitted to the wheels through a 6-speed automatic gearbox. The detailed parameters of each component are listed in Table 1. As can be easily found, there exists four operation modes in the studied PHEV, i.e., the electric driving mode, hybrid driving assist (HDA) mode, hybrid driving charge (HDC) mode and engine driving mode. The detailed descriptions of these four modes are illustrated in Table 2. As can be observed, the clutch control signal 1 denotes that the clutch is engaged, and the signal 0 means it is disengaged. The engine on=1 represents the engine starts to operate and likewise, the engine on=0 means engine is turned off. The electric motor control signal 1, 2 and 0 means that the motor operates in the tractive mode, regenerative mode and idling mode, respectively.

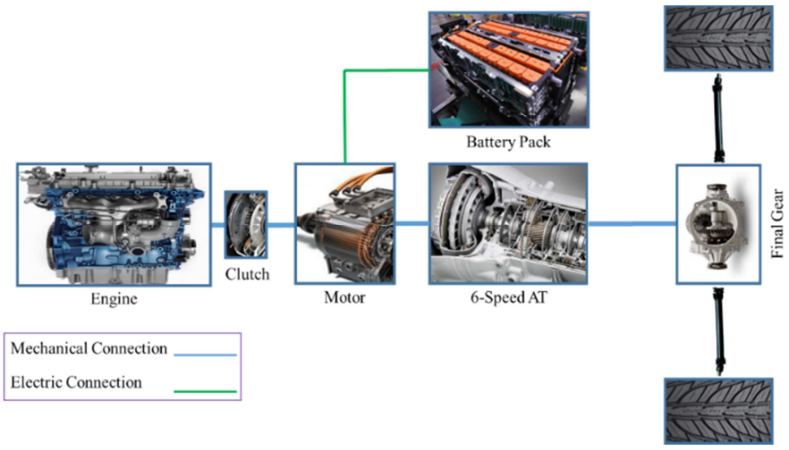


Fig. 4. The schematic of the parallel PHEV configuration.

Table 1 Specifications of Components

Components	Variable	Values
Engine	Type	In-line four-cylinder petrol engine
	Displacement	2.0 L
	Maximum Power	103 kW @6200 rpm
	Maximum Torque	270 Nm @2500~6000 rpm
Motor	Maximum Power	124 kW
	Maximum Torque	305 Nm
	Maximum Speed	12480 rpm
Battery	Type	Lithium-ion battery
	Capacity	21 Ah /6.7 kWh
	Nominal Voltage	300 V
Generator(Starter)	Maximum Power	8.5 kW
	Maximum Torque	45 Nm
Gearbox	Type	6-Speed AT

Table 2 Description on different operation modes

Mode	Component Status	Energy Flow Path
EV Mode	Clutch=0, Engine On=0, Electric Motor Mode=1,	Battery-Motor-6AT-final drive-wheels
HDA Mode	Clutch=1, Engine On=1, Electric Motor Mode=1,	Battery-Motor-6AT-final drive-wheels; Engine-Clutch-6AT-final drive-wheels;
HDC Mode	Clutch=1, Engine On=1, Electric Motor Mode=2	Engine-Clutch-6AT-final drive-wheels; Engine-Clutch-Motor-Battery;
Engine Mode	Clutch=1, Engine On=1, Electric Motor Mode=0	Engine-Clutch-6AT-final drive-wheels;

2.2.2 Mathematic Model of Parallel PHEV

The tractive force ordered by the driver is transmitted to wheels to overcome the driving resistance. The power balance equation can be formulated as:

$$P_{req}=\frac{v}{\eta_t}\left(\frac{Gf\cos\alpha}{3600}+\frac{G\sin\alpha}{3600}+\frac{C_D A v^2}{76140}+\frac{\xi ma}{3600}\right) \tag{1}$$

where P_{req} is the required tractive power; G, a and f denote the gravity, gradient and rolling resistance factor; C_D, A and v are the aerodynamic drag factor, frontal area and vehicle speed; a means the acceleration; and ξ, η_t and m represent the correction coefficient of rotating mass, transmission efficiency, and vehicle mass, respectively. At wheels, the torque balance equation can be expressed as:

$$T_{req}=T_{fuel_path}+T_{ele_path} \tag{2}$$

where T_{req} is the required tractive torque; and T_{fuel_path} and T_{ele_path} are the tractive torque provided by the fuel path and electric path, respectively. In different operating modes, the tractive force transmitted to wheels can be calculated as:

$$F_t=\begin{cases}\dfrac{(T_{eng}+T_{em})i_{gb}(n_g)i_{fd}\eta_t}{R_{wh}} & S_{clu}=1\\ \dfrac{T_{em}i_{gb}(n_g)i_{fd}\eta_t}{R_{wh}} & S_{clu}=0\end{cases} \tag{3}$$

where T_{eng} and T_{em} denote the engine and electric motor torque; i_{gb} and i_{fd} are the gear and final drive ratio, respectively; n_g is the gear number, and R_{wh} is the wheel radius. In (3), $S_{clu}=1$ means the clutch is engaged, and in contrast $S_{clu}=0$ denotes the clutch is disengaged. A static model based on an efficiency map acquired from the benchmark test is adopted to describe the nonlinear performance of engine. The following equation characterizes the relationship between the engine net efficiency and torque, as:

$$\eta_{eng}\left(T_{eng},n_{eng}\right)=\frac{T_{eng}\omega_{eng}}{Q_{lhv}\dot{m}_f} \tag{4}$$

where η_{eng} denotes the engine net efficiency, ω_{eng} means the rotating speed of engine, Q_{lhv} represents the fuel lower heating value, and $\dot{m}_f$ expresses the fuel consumption rate.

A permanent magnet synchronous motor (PMSM) is equipped in the vehicle. Since the

Journal Pre-proof

optimization target in this study is the fuel economy, the dynamic characteristic of motor is neglected due to its fast transient response. Likewise, a static model is also employed to represent the power performance of electric motor. In the parallel PHEV, the electric motor can operate as the tractive motor and generator, the relationship between the motor torque and power can be expressed as:

$$P_{em} = \begin{cases} \dfrac{T_{em}\omega_{em}}{\eta_{mot}} & T_{em} > 0 \\ T_{em}\omega_{em}\eta_{gen} & T_{em} \le 0 \end{cases} \tag{5}$$

where ω_{em} is the angular speed of electric motor; P_{em} is the power of electric motor; and η_{mot} and η_{gen} denote the efficiency in tractive mode and generator mode, respectively.

For ease of modelling the battery, the temperature and ageing influence is neglected, and a simple equivalent circuit model is employed to characterize the battery electrical performance. The model consists of an open circuit voltage source, nonlinearly varying with the SOC, and an internal resistor connecting in series topology. By simply analyzing the model of battery, the battery current, i.e., the deviation of SOC, can be calculated as:

$$\dot{SOC} = -\frac{V_{oc} - \sqrt{V_{oc} - 4R_{int}P_{batt}}}{2R_{int}Q_{batt}} \tag{6}$$

where SOC is the battery SOC, V_{oc} is the open circuit voltage of battery, R_{int} is the internal resistance of battery, P_{batt} is the battery power, and Q_{batt} is the battery capacity.

III. The Cooperative Control Strategy for the PHEV

The presented cooperative control strategy includes two stages. The energy management will be executed by vehicle components after energy allocation plan and utilization management. The optimal battery SOC trajectory and velocity profile of future travel in each route segment are generated in MECs and sent to the on-board VCU of target vehicle. The MPC based method tracks the optimal battery SOC trajectories and velocity profiles to regulate the energy flow between the engine and battery. The approximate implementation process of the strategy is illustrated in Fig. 5.

As can be seen, in the stage of energy utilization plan, the IDP can generate optimal battery SOC trajectories with faster calculation speed, compared with the deterministic DP. However, the narrowed optimization horizon for fast computation, from the whole route to the route segment, prevents the

Journal Pre-proof

control effect from global optimum. The difference is attributed to the running global optimization in route segment without chance of previewing the overall driving conditions in the whole trip. Furthermore, global optimization algorithms integrally consider variation of driving conditions in each route segment, imposed on the total fuel consumption, by intelligently governing more electric energy to be consumed in some route segments. To compensate the performance gap between that of the proposed method implemented in each route segment and of the global optimization based method (deterministic DP) performed on the whole trip, the allowed electric energy consumption in each route segment is quantitatively planed according to different driving conditions. The velocity profile of future trip in each route segment is predicted according to the shared traffic data from the volunteer vehicles on route with the full consideration of traffic macroscopic behaviors and security. The terminal states of former route segment will be sent to the MECU that is responsible for the subsequent route segment. In addition, the MECU that is in charge of current route segment plans the optimal reference for next route segment. In the stage of energy utilization management, the MPC based method distributes the demanded energy between the engine and battery by tracking the planned optimal battery SOC trajectory according to the predicted velocity profiles in short horizon with the optimized calculation steps. The MPC based solutions guarantee the dynamic adaption to traffic conditions and optimal performance. The detailed description about the algorithms will be discussed in the following parts.

Journal Pre-proof

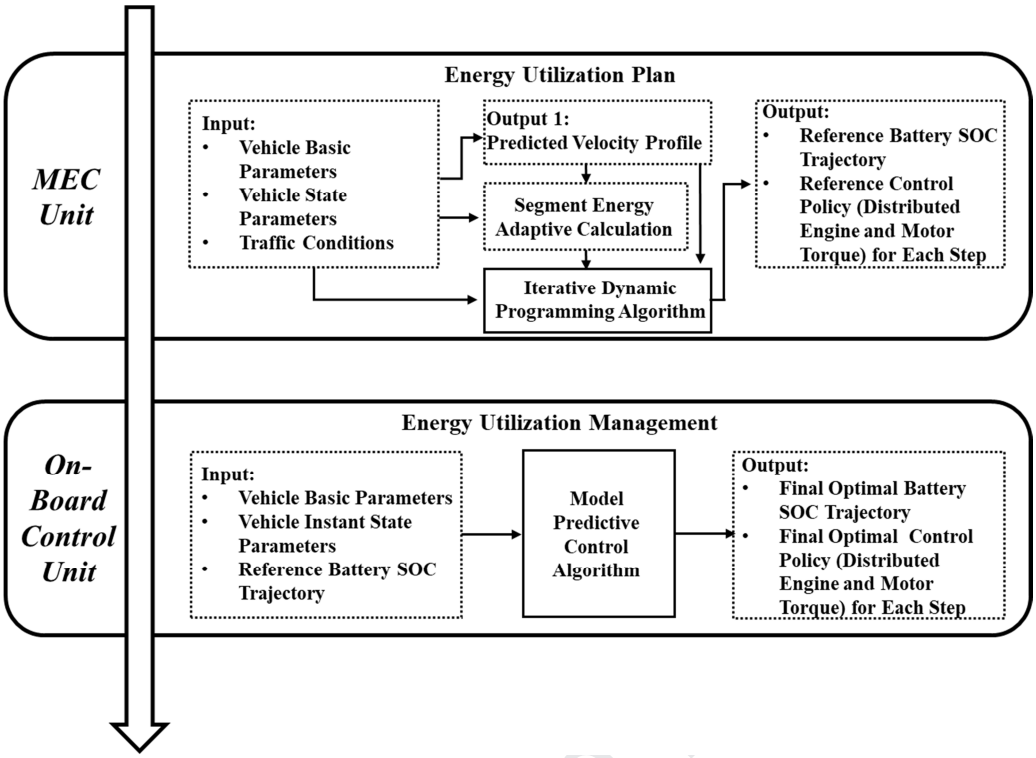


Fig. 5. The general description on the cooperative control strategy.

3.1 Energy Utilization Plan by IDP

3.1.1 IDP Method Derived from Deterministic DP

DP is applied to find the optimal control policies as the reference in energy utilization plan stage, and it contains a two-stage calculation process to finalize the optimization. In the first stage, a so-called backward calculation is conducted from the end of driving cycle to the beginning under the setting constraints of variables and terminal state. At the discrete step k in backward calculation, the cost-to-go values, from each discrete state variables to the set terminal state, are accumulated after assigning a series of discrete control variables, as shown in Fig. 6. The cost-to-go function can be expressed as:

$$J_k(x_k^i) = \left\{ h_k(x_k^{io}, u_k^j) + J_{k+1}(F_k(x_k^{io}, u_k^j)) \right\} \tag{7}$$

where x_k^i and u_k^j mean the i th state and control variable at step k, respectively; h_k is the stage cost for the transition from x_k^i to the state at step $k+1$ after assigning the control variable u_k^j, F_k is the state function to describe the state transition. In this process, some errors may arise due to the discrete grid sizes of state and control values; therefore, the interpolation is suggested to search the more

precise cost-to-go value J_{k+1} for step $k+1$, as highlighted with the red dash line in Fig. 6. In the forward calculation, the optimal control policies are chosen according to the optimal cost-to-go values for each state. Similarly, the interpolation is also required for the errors incurred by the discrete grid size. With regard to the optimization problem in PHEVs, the stage cost function represents the total fuel consumption.

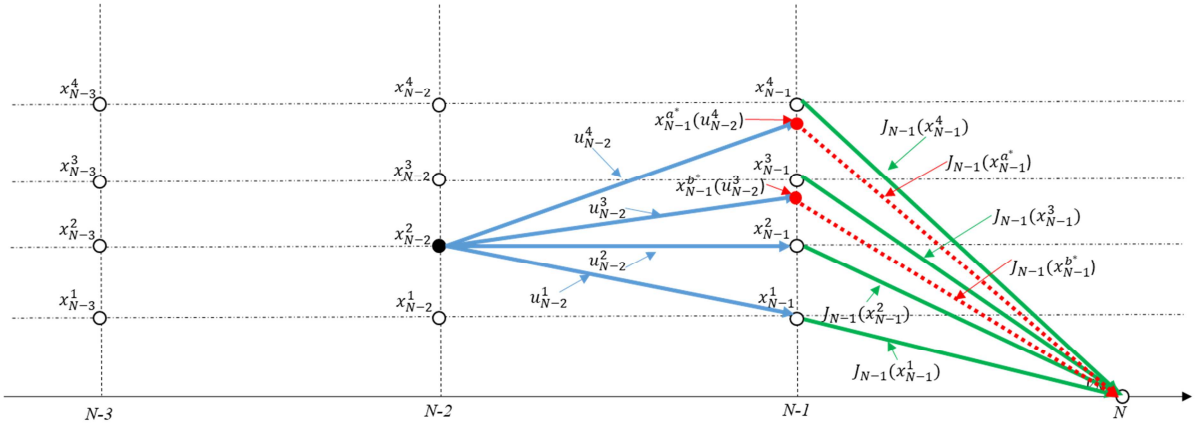


Fig. 6. Process of backward calculation in DP.

Table 3 The pseudocode of IDP algorithm

1	Initialization
2	Do {
3	Run the deterministic *DP*
4	Save optimal state trajectory and control vectors of iteration q
5	Adjust constraints on state and control vectors
6	Adjust grid sizes of state and control vectors
7	$q = q+1$
8	} Until $q = N_i$ (N_i : the iteration times)

The deterministic DP algorithm can provide the optimal solution and also demands large computation intensity, as it calculates the cost-to-go value of each discrete state under different control variables at each step, thus leading to massive processor memory. For the deterministic DP problem with k steps, by assuming that the grid size of state variable and control state variable at each step are respectively m and n; we can deduce that the calculation complexity will be m^2n^2k . Apparently, grid sizes of the state and control variable are critical to determine the calculation speed. Finding effective manners is highly encouraged to decrease grid sizes of control variable and state

variable in DP while ensuring optimization. Meanwhile, coarse grid sizes may discount the controlling effect. The emerging IDP provides a new manner to mitigate the discussed problem. As a numerical method, IDP can save the calculation time and still attain the comparable optimal effect solved by the deterministic DP with smaller amount of state and control variables [26]. In each iteration, grid sizes of state and control variable will be adjusted to keep the lowest request on processor memory. The pseudocode of IDP algorithm is provided in Table 3, and the illustration of the IDP implementation process is provided in Fig. 7. Another advantage of IDP is that the adaptive adjustment in each iteration can be made according to the pre-set constraint target, extending the application scenario. Ref. [38] tries to guarantee the travel time by a weight value adjustment function when applying the IDP to generate optimal velocity profiles. Inspired by the work introduced in [38], the energy consumption in each route segment can be adjusted, thus making it possible that the result of energy utilization plan in each route segment is close to that by global optimization in the whole trip. To the best of authors' knowledge, IDP has not been exploited in energy management with active adjustment in previous research.

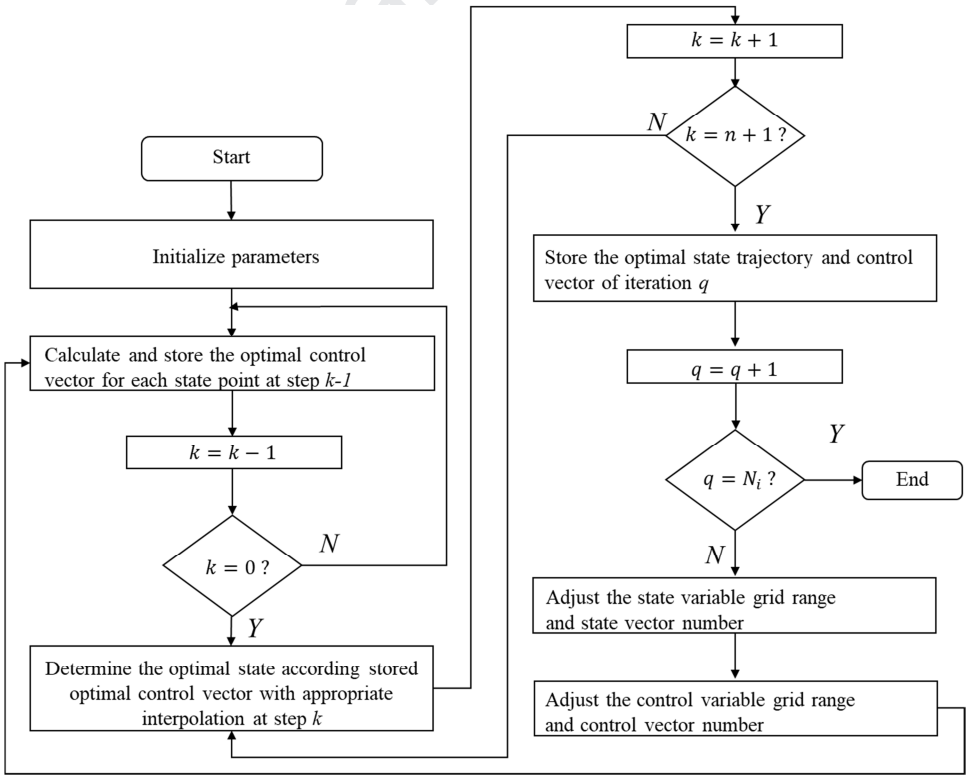


Fig. 7. Illustration of the IDP implementation.

3.1.2 Implementation of IDP in Energy Utilization Plan

Journal Pre-proof

As described above, the aim of energy utilization plan is to generate the optimal battery SOC trajectory in each route segment by means of the IDP. The state variable when applying the IDP for energy utilization plan is the battery SOC, which is also the optimization target; and the control variable is the power distribution ratio between the engine and battery. By optimizing the power distribution ratio, the optimal battery SOC variation in each step can be determined by (8). Actually, the optimal battery SOC trajectories is the another form of the optimal control policy (power distribution ratio μ). The optimal control policy stems from the iterative optimization process in IDP with the target of minimizing the energy consumption. Therefore, the optimal variation of SOC will lead to better energy efficiency. The stage cost function h_k can also be expressed in (8), as:

$$\begin{cases} h_k = \dot{m}_f(x_k, u_k) + \omega_t \dfrac{P_{batt}}{Q_{lhv}} \\ P_{batt} = \dfrac{P_{em}}{\eta_{ele}} \\ \Delta SOC = \dfrac{2 \cdot P_{batt} \cdot \Delta s}{3.6 \cdot Q_{batt} \cdot \left(v(k) + v(k+1)\right)} \end{cases} \tag{8}$$

where s denotes the simulation step in the distance domain, η_{ele} is the electric energy transmit efficiency, and ω_t is the weight on electric energy consumption, which can be calculated as:

$$\omega_t(q+1) = \omega_t(q) + sign\left(E_{e_real}(q) - E_{e_target}(q)\right) \times \delta e^{\left(E_{e_real}(q) - E_{e_target}(q)\right)^2} \tag{9}$$

where q is the iteration time, E_{e_real} is the real electric energy consumption in the qth iteration, E_{e_target} is the target electric energy consumption, and is a constant. By introducing ω_t, the electric energy consumption in each route segment can be actively regulated. In terms of the IDP implementation, the related functions of adjusting the grid sizes of state and control variable can be expressed as:

$$\begin{cases} x_{k_min}^{q+1} = max(x_{k_min}^{q}, x_{k_{opt}}^{q} - \alpha(x_{k_\max}^{q} - x_{k_min}^{q})) \\ x_{k_\max}^{q+1} = \min(x_{k_\max}^{q}, x_{k_{opt}}^{q} + \alpha(x_{k_\max}^{q} - x_{k_min}^{q})) \\ u_{k_min}^{q+1} = max(u_{k_min}^{q}, u_{k_{opt}}^{q} - \beta(u_{k_\max}^{q} - u_{k_min}^{q})) \\ u_{k_\max}^{q+1} = \min(u_{k_\max}^{q}, u_{k_{opt}}^{q} + \beta(u_{k_\max}^{q} - u_{k_min}^{q})) \end{cases} \tag{10}$$

where $x_{k_\max}^{q+1}$ and $x_{k_min}^{q+1}$ denote the upper and lower boundaries of state variables at step k in iteration $q+1$; $x_{k_{opt}}^{q}$ and $u_{k_{opt}}^{q}$ are the optimal state and control variable at step k in iteration q; $u_{k_\max}^{q}$ and $u_{k_min}^{q}$ are the upper and lower boundaries of control variables at step k in iteration q; and α and β are the contracted ratios, respectively. Moreover, the implementation of IDP should also satisfy the inequality constraints from powertrain components and vehicle dynamic. To reduce the computation burden, except applying the variable and boundary functions in (10), the energy utilization plan is narrowed within each route segment rather than the global trip. Shrinking scope of the optimization may deteriorate the controlling effect as the optimization process switches into local optimization. To bridge the gap between the proposed method and global optimization method, electric energy consumption should be rationally planned by (8) and (9). Particularly, E_{e_target} can be calculated as:

$$E_{e_target}^{i} = T_f^{i} \times E_{e_basic}^{i},\ i = 1,2,3,\ldots,n \tag{11}$$

where i denotes different route segment, and T_f is the traffic factor, as:

$$T_f = \frac{v_{ave}}{v_{std}} \tag{12}$$

where v_{ave} is the average speed in certain route segment, and v_{std} is the velocity standard deviation in certain route segment. In (11), E_{e_basic} is the estimated electric energy consumption according to the predicted velocity profile for the route segment. Methods to predict the velocity profile according to the shared traffic information has been discussed in our previous work [39]. The velocity profile prediction method detailed in [39] is a macroscopic method that considers the impact from weather and traffic condition. The future velocity is predicted based on the shared data from volunteer vehicles on the routes, which includes geographic information and vehicle speeds. The shared vehicle speed is the direct result of driving behavior of each vehicle with fully considering safe distance to forward vehicles and weather conditions. In this study, E_{e_basic} can be calculated as:

$$E_{e_basic} = \int P_{req}(v(s)) - \eta_t \cdot P_{eng_{opt}}(v(s)) \cdot ds \tag{13}$$

where $P_{eng_{opt}}$ is the engine power corresponding to the optimal operation points in brake-special fuel consumption (BSFC) line at a certain velocity. The method of calculating E_{e_target} is inspired by the simulation analysis. Fig. 8 presents the battery SOC trajectories supplied by the deterministic DP on routes with different T_f. As can be seen, larger T_f leads to lower terminal battery SOC, revealing more electric energy consumption.

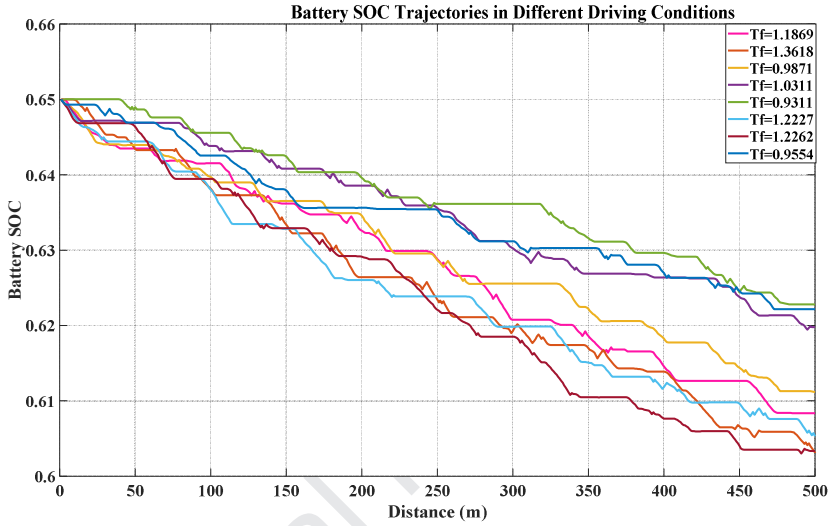


Fig. 8. Battery SOC trajectories by DDP on routes with different T_f

3.2 Energy Utilization Management by MPC

After completing the energy utilization plan in MECUs, the optimal battery SOC trajectories for the chosen travel route will be transmitted to the on-board VCU. The control algorithm in VCU, i.e., MPC method, will tackle the energy management by tracking the optimal battery SOC trajectory. In this study, the nonlinear MPC based instantaneous optimization method is still in a distance domain. Different from the optimization process in MECUs, the calculation step in the nonlinear MPC is reduced to 2 m and the horizon length for the receding optimization is set to 10 m. The fining calculation step can ensure the optimization more reliable and efficient within limited computation time. The step number in the receding optimization is supposed to 5 accordingly. The calculation step of IDP in MECUs is 10 m, and therefore interpolation on the optimal battery SOC trajectory is indispensable. In addition to tracking optimal trajectories, the velocity profiles generated in MECUs are also requested to follow for adaption to traffic conditions.

3.2.1 General Control Problem Formulation in MPC

In general, the optimal MPC problem in the distance domain to minimize the given cost function can be expressed as:

$$J = H(x(s_f), u(s_f), s_f) + \int_0^{s_f} L(x(s), u(s), s)ds \tag{14}$$

where x and u are the state and control inputs, respectively; s is the distance step; s_f is the terminal state; H is the terminal cost; and L is the stage cost. The optimal control problem is subject to the given inequality constraints:

$$\begin{cases} x_{\min} \le x(s) \le x_{\max} \\ u_{\min} \le u(s) \le u_{\max} \\ g\left(x(s), u(s), s\right) \le 0 \end{cases} \tag{15}$$

The equality constraint is the ordinary differential equation (ODE), as:

$$\dot{x}(s) = f\left(x(s), u(s), s\right) \tag{16}$$

To sum up, the described optimal control problem in (14)-(16) becomes a nonlinear programming problem (NLP) after discretization and parametrization. To realize the optimal tracking based on MPC algorithm, the problem can be reformulated as:

$$U^*(k) = \arg\min \sum_{i=1}^{n_p} \left\| y(k+i) - y^*(k) \right\|_Q^2 + \left\| \Delta u(k+1) \right\|_R^2 \tag{17}$$

subject to:

$$\begin{cases} x(k+1) = Ax(k) + Bu(k) \\ u(k) = u(k-1) + \Delta u(k) \\ y(k) = Cx(k) + Du(k) \\ u_{\min} \le u(k) \le u_{\max} \\ x_{\min} \le x(k) \le x_{\max} \\ y_{\min} \le y(k) \le y_{\max} \end{cases} \tag{18}$$

where y is the control output, Q and R are the penalty matrixes, and n_p is the prediction length. In (18), the controlling inputs in the prediction horizon can be expressed as:

$$\begin{cases} U(k) = \left[\Delta u^T(k), \Delta u^T(k+1), \Delta u^T(k+2), \ldots \Delta u^T(k+n_c) \right]^T \\ \Delta u(k+i) = \Delta u(k+n_c - 1), i = n_c, \ldots n_p \end{cases} \tag{19}$$

where n_c is the control horizon. The ODE in (16) can be rewritten as:

$$\begin{cases} x(k+1) = A_e x(k) + B_e A_n^{N_p-1} u(k) \\ y(k) = C_e x(k) \end{cases} \tag{20}$$

where A_e, B_e, and C_e are parameter matrixes. The states and control outputs in the prediction horizon can be acquired by (21) and (22), as:

$$\hat{y} = \begin{bmatrix} C_e A_e \\ C_e A_e^2 \\ \vdots \\ C_e A_e^{N_{p_e}} \end{bmatrix} x(k) \tag{21}$$

$$\hat{x} = \begin{bmatrix} A_e \\ A_e^2 \\ \vdots \\ A_e^{N_{p_e}} \end{bmatrix} x(k) + \begin{bmatrix} B_e \\ A_e B_e \\ \vdots \\ A_e^{N_{p_e}-1} B_e \end{bmatrix} \hat{u} \tag{22}$$

In (21) and (22), $\hat{y}$, $\hat{x}$, and $\hat{u}$ can be expressed as:

$$\begin{cases} \hat{y} = \begin{bmatrix} y(k+1) \\ \vdots \\ y(k+N_{p_e}) \end{bmatrix} \\ \hat{u} = \begin{bmatrix} u(k) \\ \vdots \\ u(k+N_{c_e}) \end{bmatrix} \\ \hat{x} = \begin{bmatrix} x(k+1) \\ \vdots \\ x(k+N_{p_e}) \end{bmatrix} \end{cases} \tag{23}$$

Accordingly, equations (21) and (22) can be revised as:

$$\begin{cases} \hat{y} = \Theta x(k) \\ \hat{x} = \Phi x(k) + \Psi \hat{u} \end{cases} \tag{24}$$

where Θ, Φ, and Ψ are the resulting matrixes. The optimal tracking problem in (17) can be reformulated as:

$$\min J = \min\left(\hat{y}^T Q_1 \hat{y} + \hat{x}^T Q_2 \hat{x} + \hat{u}^T R \hat{u}\right) \tag{25}$$

subject to:

$$\left(x(k+i),u(k+i)\right)\in \aleph, i=0,\ldots,n_p \tag{26}$$

where Q_1, Q_2 and R are penalty matrixes, and $\aleph$ is the prediction set. Substituting (24) into (25) and dividing by 2, the optimal tracking problem in (25) can be rewritten into a quadratic programming (QP) problem:

$$\min J = \min\left(\frac{1}{2}\hat{u}^T(\Psi^T Q_2 \Psi + R)\hat{u} + x(k)^T \Phi^T Q_2 \Psi \hat{u}\right) = \min\left(\frac{1}{2}\hat{u}^T S\hat{u} + x(k)^T W\hat{u}\right) \tag{27}$$

subject to:

$$P\hat{u} \le M_1 + M_2 x(k) \tag{28}$$

where S, W, P, M_1 and M_2 are the constant matrix.

3.2.2 MPC Controller Design for Energy Utilization Management

The MPC controller is requested to track the predicted velocity profiles and generated optimal battery SOC trajectories released from MECU. By following the two trajectories, energy management can be ultimately completed, thereby guaranteeing the final controlling effect is close to the reference. In the tracking process, the predicted velocity profiles offer approximate control environment with that in the energy plan stage, and the optimal battery SOC trajectories provide the controlling reference. Therefore, the predicted velocity profiles and optimal battery SOC trajectories are two constraints in the MPC application. The total tractive torque T_{req} at wheels and the power distribution ratio μ between the engine and motor are the control inputs (control variables) to govern the two control outputs (state variables): vehicle speed and battery SOC. In the parallel PHEV, the relationship between T_{req} and velocity can be expressed as:

$$\dot{v}(k) = \frac{1}{m}\left(T_{trac}(k) - \frac{1}{2}C_D A v^2(k) - mgf\cos\theta(k) - mg\sin\theta(k)\right) = \frac{1}{m}\left(T_{req}(k) - P_1 v^2(k) - P_2\right) \tag{29}$$

where $P_1 = \frac{1}{2}C_D A$, $P_2 = mgfcos\theta(k) + mgsin\theta(k)$, and g is the gravity acceleration. In the distance domain calculation, the velocity at next location can be described as:

$$v(k+1) = v(k) + \dot{v}(k)\frac{2\Delta s}{v(k)+v(k)} \tag{30}$$

where Δs is the calculation step, and k and $k+1$ denote the current step and next step. By combining (30) and (29), the relationship between the control input and velocity can be obtained, as:

$$v(k+1)^2 = (1-\frac{2\Delta s}{m}P_1)\cdot v(k)^2 + \frac{2\Delta s}{m}T_{req}(k) - \frac{2\Delta s}{m}P_2 = Av(k)^2 + BT_{req}(k) - C \tag{31}$$

where $A = 1-\frac{\Delta s}{m}C_D A$, $B = \frac{2\Delta s}{m}$, and $C = \frac{2\Delta s}{m}\left(mgfcos\theta(k) + mgsin\theta(k)\right)$. In the receding optimization by MPC algorithm, the optimal T_{req} sequence is searched to guarantee the real velocity profiles close to the predicted ones. Corresponding to each T_{req}, P_{req} at each time interval can be calculated by (1). Then the relationship between the power distribution ratio and battery SOC can be expressed as:

$$SOC(k+1) = SOC(k) + \frac{2\cdot\mu\cdot P_{req}\cdot\Delta s}{3.6Q_{batt}\cdot\left(v(k)+v(k+1)\right)} \tag{32}$$

The cost function described in (17) can be formulated for the energy unitization management, as:

$$J_c(k) = \omega_1\sum_{i=1}^{n_p}\left(v(i|k) - v_{opt}(i|k)\right)^2 + \omega_2\sum_{i=1}^{n_p}\left(SOC(i|k) - SOC_{opt}(i|k)\right)^2 \tag{33}$$

Meanwhile, it should be subject to:

$$\begin{cases} SOC_{min} \le SOC \le SOC_{max} \\ P_{batt_min} \le P_{batt} \le P_{batt_max} \\ T_{em_min} \le T_{em} \le T_{em_max} \\ T_{eng_min} \le T_{eng} \le T_{eng_max} \\ \omega_{em_min} \le \omega_{em} \le \omega_{em_max} \\ \omega_{eng_min} \le \omega_{eng} \le \omega_{eng_max} \end{cases} \tag{34}$$

where v_{opt} and SOC_{opt} are the optimal velocity and battery SOC trajectories from MECUs, and the subscripts *min* and *max* denote the minimum and maximum value of each variable, respectively. To solve the defined QP problem, ACADO, a toolkit in Matlab, is preferred in this paper for simulation [40, 41].

IV. Simulation and Evaluation

The simulation test is performed on a workstation with an Intel Xeon E3-1270 @ 3.4 GHz with 32 Gb memory. Two travel routes are selected in the comparative test. To better demonstrate the

Journal Pre-proof

energy utilization plan and management by the proposed method, the randomly chosen travel routes reflect the complicated city urban driving conditions. The total length of each travel route is 4.5 km, in which three MECUs are implemented, and each MECU is responsible for the workload of 1.5 km. The initial battery SOC is set to 0.65. Based on the geographic information of selected travel routes, the velocity profiles of vehicle in two routes can be predicted.

4.1 Compare Analysis of Performance in Energy Utilization Plan

With respect to the simulation results, DP refers to that application of the deterministic DP on the whole travel route. DP-Seg means applying the deterministic DP in each route segment without any energy consumption adjustment. IDP-Seg represents applying the IDP method in each route segment with the corresponding permitted energy consumption adjustment. DP-Seg is a candidate to accelerate the energy plan. Owning to the narrowed optimization scope within route segment and without any adaptive adjustment, the energy plan effect by DP-Seg may be worse than that by DP conspicuously. Consequently, DP-Seg is an effective algorithm that highlights the superior performance of IDP-Seg in energy plan. To better evaluate and analyze the simulation results, a number of points in certain figures are labelled, representing the active adjustment by the IDP strategy. Fig. 9 exhibits the predicted velocity profiles of two driving routes according to the shared traffic data in MECUs. The two travel routes feature the city urban driving conditions with frequently changed velocity and widely varying acceleration. Table 4 lists the traffic factor values of each route segment.

Journal Pre-proof

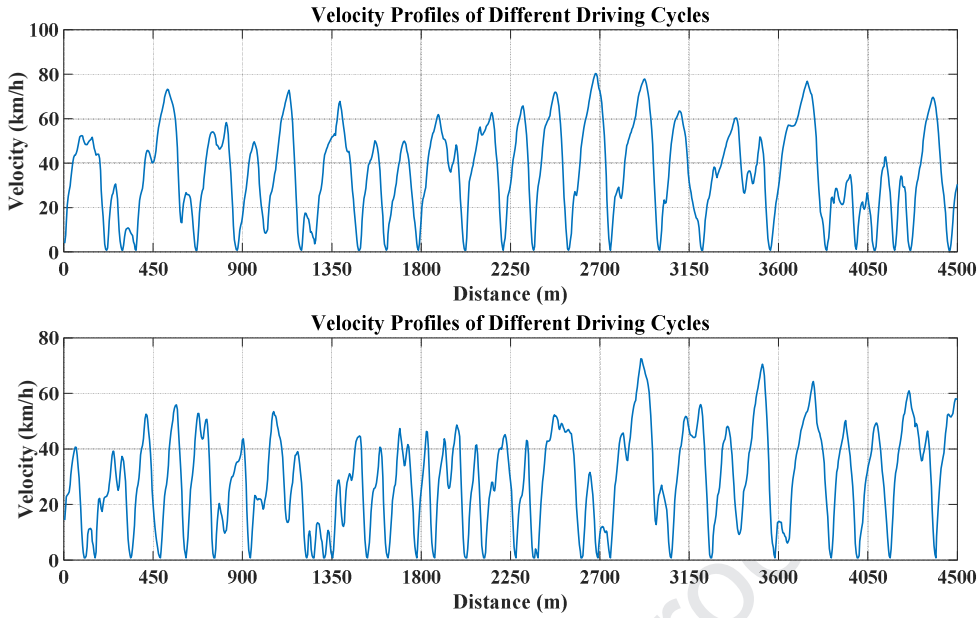


Fig. 9. Predicted velocity profile in two travel routes.

Table 4 Traffic factors of different route segment

Travel Route	Route Segment	Traffic Factor	Average Speed (m/s)	Average Travel Time (s)
1	R1	1.187	4.562	328.8031
	R2	1.362	5.708	262.7891
	R3	0.987	3.697	405.7344
2	R1	1.031	3.035	494.2339
	R2	0.931	3.179	471.8465
	R3	1.226	4.669	321.2679

4.1.1 Brief Analysis on the Simulation Results

As clearly shown in Fig. 10 and Table 5, the fuel and electric energy consumption solved by IDP-Seg is much close to that based on the deterministic DP, thereby roughly verifying that the proposed method can achieve better performance than DP-Seg. The superior performance in energy consumption and computational effort verify the capability of the proposed method in quantified fast global optimization.

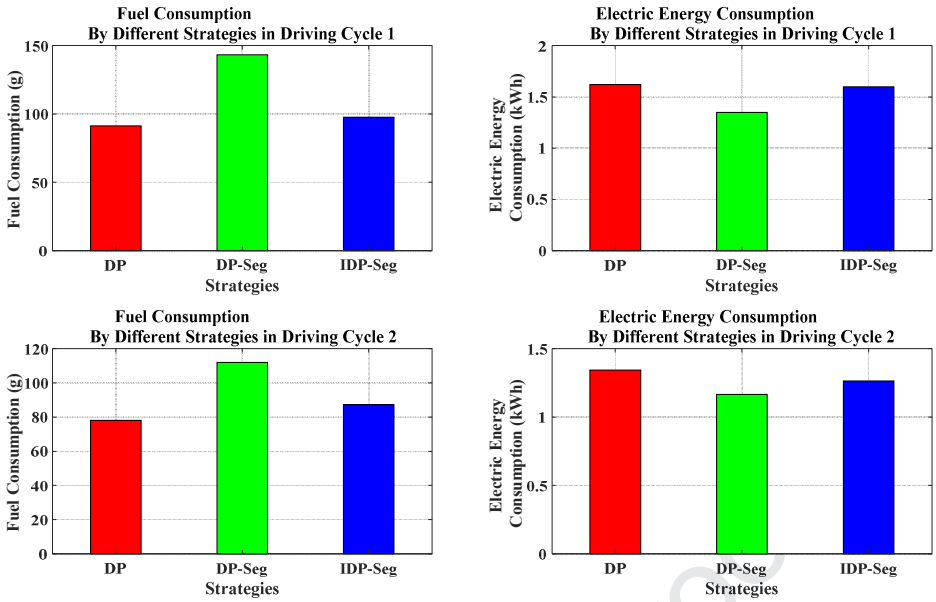


Fig. 10. Energy consumption comparison in whole travel route by different methods.

Table 5 Energy consumption in the whole travel route by different strategies

Travel Route	Control Strategy	Total Fuel Consumption (g)	Total Fuel Consumption (L/100km)	Total Electric Energy Consumption (kWh)
1	DP	91.26	2.79	1.62
	DP-Seg	143.19	4.38	1.34
	IDP-Seg	97.61	2.99	1.59
2	DP	78.09	2.39	1.34
	DP-Seg	112.05	3.43	1.16
	IDP-Seg	87.26	2.67	1.26

4.1.2 Further Evaluation on Simulation Results

Based on the general conclusion made in the previous section, further evaluation is conducted to investigate the principle in performance improvement of the proposed method. Table 6 lists the detailed energy consumption in each route segment. According to the traffic factors provided in Table 4 and the results listed in Table 6, the IDP-Seg can lead to more electric energy consumption, compared with DP-Seg, if the traffic factor value is greater than one. In contrast, the IDP-Seg allows less electric energy consumption if the traffic factor value is less than one. The active adjustment can be made depending on whether the conditions favor more electric energy to be consumed. By rationally controlling the motor operation, the engine operation region is limited within high efficiency fields, resulting in less fuel consumption. Owing to the special characteristics of IDP, the energy consumption can be planned, and hence the proposed method can achieve more approximate

Journal Pre-proof

behaviors to that by DP.

Table 6 Energy consumption in each segment by different strategies

Travel Route	Control Strategy	Route Segment	Fuel Consumption (g)	Electric Energy Consumption (kWh)
1	DP-Seg	R1	45.92	0.43
		R2	72.09	0.48
		R3	25.18	0.43
	IDP-Seg	R1	30.04	0.51
		R2	40.87	0.66
		R3	26.70	0.42
2	DP-Seg	R1	34.87	0.35
		R2	35.44	0.32
		R3	41.74	0.49
	IDP-Seg	R1	29.74	0.36
		R2	36.55	0.29
		R3	20.97	0.61

Figs. 11 to 13 reveal the concrete adjustment actions supplied by IDP-Seg. Three adjustment actions are chosen and labelled. In Fig. 11, it can be found that the electric energy consumption is encouraged in first two route segments of travel route 1. The descent rate of battery SOC is larger than that by DP-Seg in the first route segment. Therefore, the HDC mode is preferred at the beginning of the second route segment (1500 m, AD1), pulling up the SOC descent rate consequently. As a result, more electric energy is consumed at the second route segment (1500 to 3000 m, AD2). This is attributed to the road conditions that aggravate the total energy consumption without more engagement of the HDA mode and EV mode. In the third route segment of travel route 1, the HDC mode is chosen to guarantee that the total electric energy consumption can meet the pre-planned requirement (3000 m, AD3). The engine torque and motor torque results depicted in Figs. 12 to 15 also support the upper analysis. At AD1, more negative motor torque is requested to lessen the decline slope of SOC. At AD2, more electric energy is consumed by frequently choosing the HDA mode. At AD3, the HDC mode is picked up again to meet the pre-planned electric energy consumption requirement. In travel route 2, less electric energy is consumed in route segment 2 (around 1800 m, AD2) and more electric energy is utilized in route segment 1 (around 0 to 1200 m, AD1) and route segment 3 (around 3000 m, AD3). The control actions are also determined according to different road conditions. The AD1 and AD2 in travel route 2 is similar to that in the second route segment and the third segment of travel route 1, whereas the AD3 is close to the first adjustment in travel route 1.

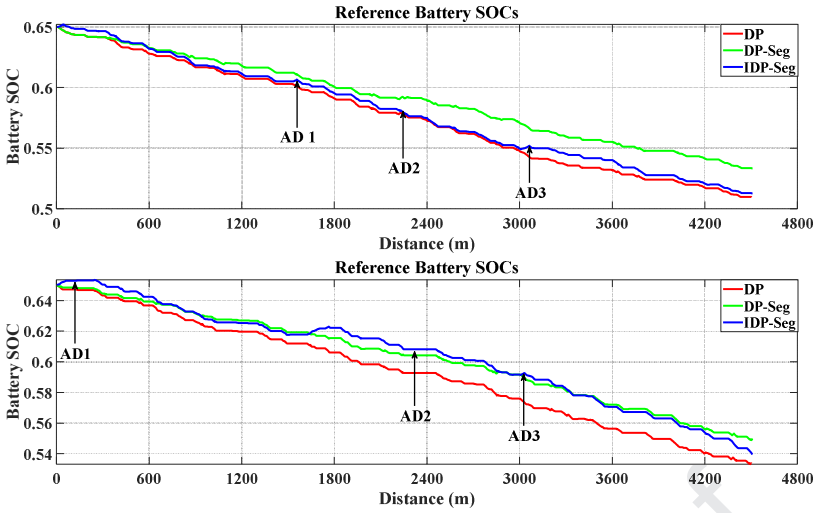


Fig. 11. Battery SOC trajectories planned by different methods for the whole travel.

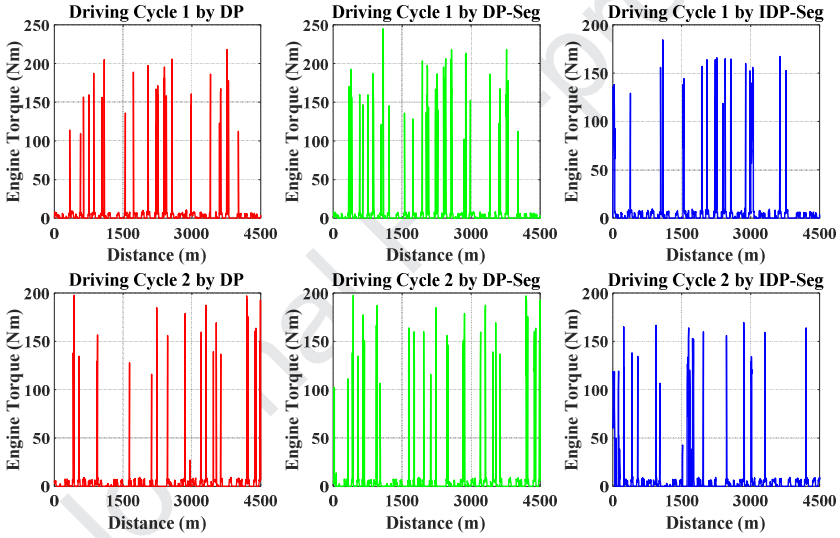


Fig. 12. Engine torque by different methods in whole travel route.

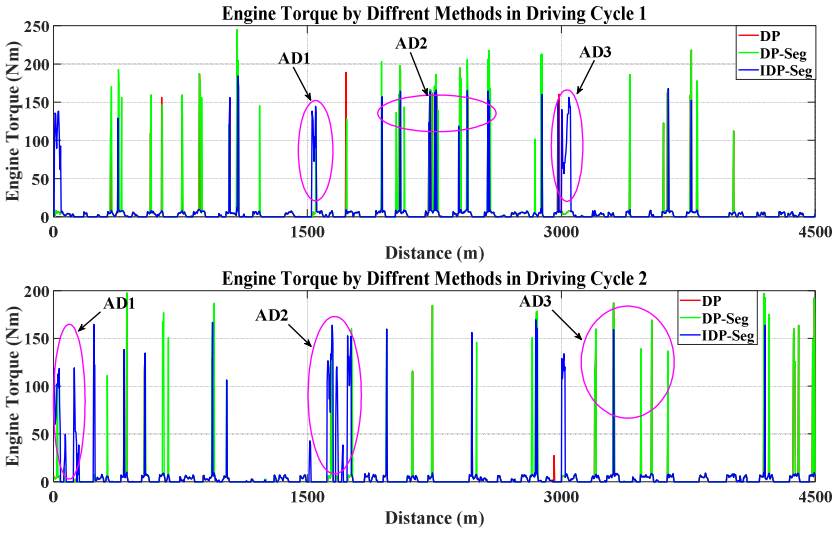


Fig. 13. Engine torque comparison by different strategies in the whole travel route.

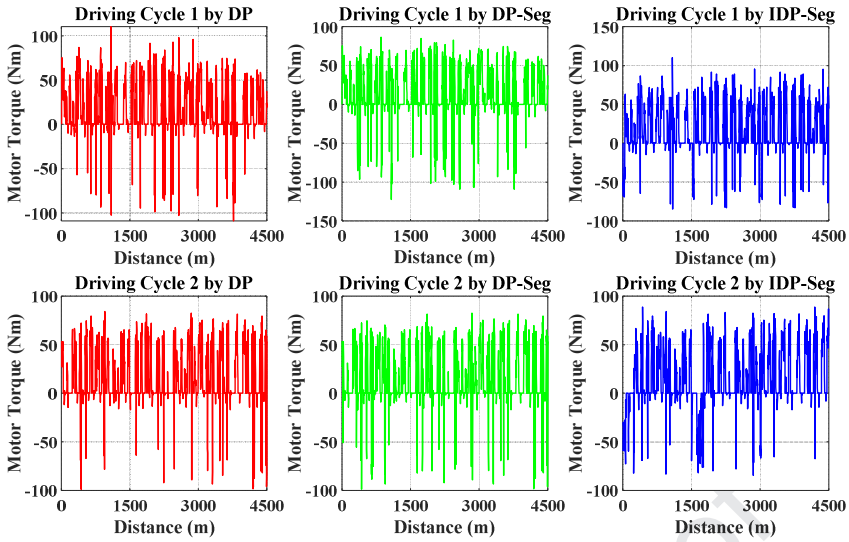


Fig. 14. Motor torque by different methods in the whole travel route.

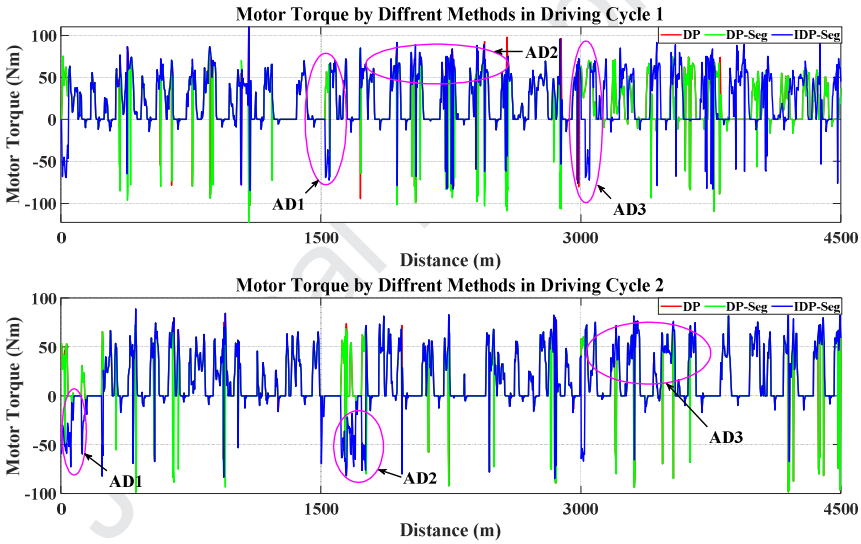


Fig. 15. Motor torque comparison by different strategies in the whole travel route.

4.2 Evaluation the Performance in Energy Utilization Management

Figs. 16 and 17 show the performance of MPC algorithm in following the reference optimal control policies acquired from MECUs. The optimization target of control algorithm is the fuel economy, and the energy consumption optimization is presented and compared. In Fig. 16, it is obvious that the MPC algorithm can track the reference SOC trajectories adequately, ensuring that the optimal control policies can be executed by the powertrain components. There exist some minor differences in the engine and motor torques, as shown in Fig. 17, when the MPC algorithm follows the optimal control policy. This may be arisen by the difference when converting the powertrain

function from nonlinear to linear manner. In the optimization control process of MPC, the required tractive torque, actually, is acquired from the look-up table according to the driving requirement. Converting this process from nonlinear states to linear states requests the curve fitting method to generate high order functions, thus causing errors consequently. In short, it can be summarized that the energy flow between the engine and battery can be rationally governed by adequately tracking the designed reference SOC trajectories. Furthermore, by means of the developed two-stage method, energy management in PHEVs can be accomplished fast with the performance that is much closer to the global optimal methods.

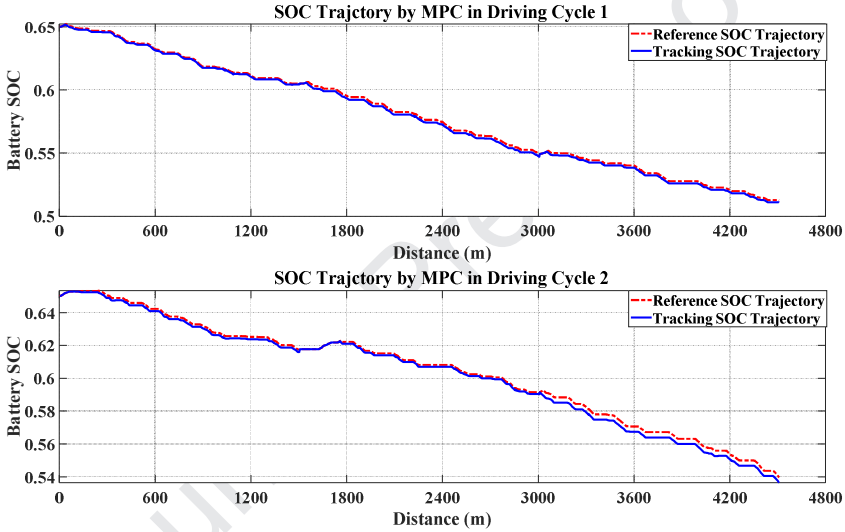
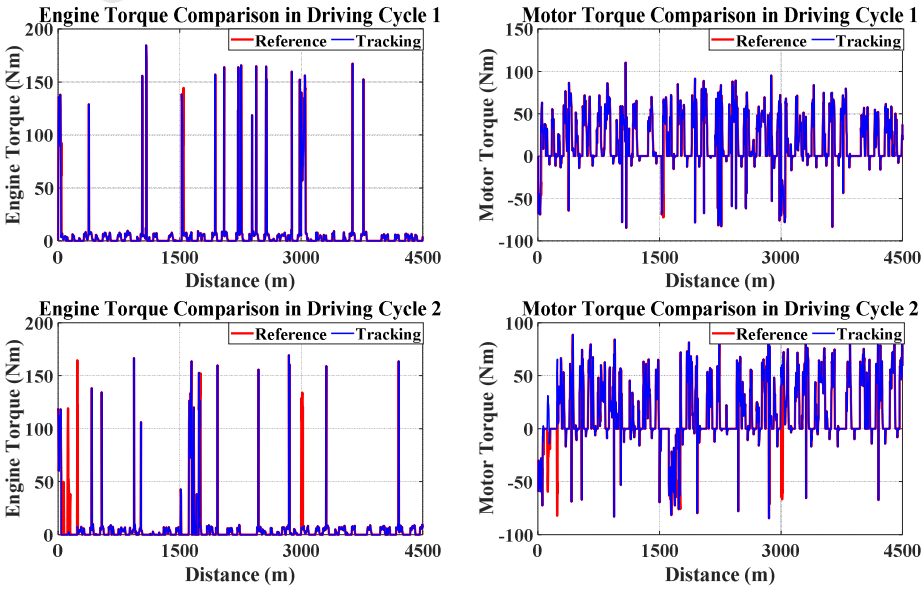


Fig. 16. Battery SOC trajectory tracking results.



Journal Pre-proof

Fig. 17. Components performance by MPC.

4.3 Evaluation of the Real-time Application Capability

To validate the real-time application capability in real time, the evaluation in terms of control process involved in energy utilization plan and energy utilization management is investigated. Since the velocity prediction method employed in this paper is a data-mining based method, the simple calculation is conducted to predict future velocity profile. Here we assume that calculation time of velocity profile prediction will not affect the total calculation time. In the energy utilization plan stage, the optimal reference for energy utilization management in first route segment can be acquired before the vehicle starts to drive in first route segment. We also assume that MECU in current route segment plans the optimal reference for next route segment. The evaluation pays attention to the following fields: communication delay, computation effort in energy utilization plan and energy utilization management.

In a MEC-based IOV system as depicted in Fig. 2, the following simulation parameters are set to calculate the delay. As a comparison, we assume that the computing capacity at the vehicle is 10 or 20 Giga CPU cycles/s, the transmission bandwidth is 10 MHz, the distance between the vehicle and BS is 20 m, the antennas number is N=8, and the computing capacity at the MEC server is F=50 Giga CPU cycles/s. The data length 0.1 Mbits, and the computing number is 0.1 Giga CPU cycles. The time delay can be directly solved by optimization methods in [42]. From Fig. 18, we find that the delay is lower than 4 ms when the edge computing is performed. Meanwhile, the delay decreases with the increment of transmit power of vehicle. In addition, from Fig. 19, one can observe that the transmit rate can reach 5.6×10^8 bit/s when the transmit power of vehicle is 20 dBm, which is enough to guarantee the data transmission. The calculation time of different methods in energy utilization plan is detailed in Table 7. According to the results listed in Tables 4 and 7, the calculation time of IDP-Seg in each route segment is shorter than the estimated travel time, proving that the raised method can be qualified for real-time application. Even though the total calculation time by DP-Seg is shorter than that by DP, the calculation time in each route segment is still longer than the estimated travel time, indicating that optimal reference plan cannot be completed before the vehicle drives into next route segment. Thus, the online application effect by DP-Seg will be hindered. Table 8 lists the calculation

time in each time step based on the MPC reference tracking manner. The calculation time in each step is a key parameter to evaluate the real-time application capability. According to the results in Table 8, the calculation time in each step in MPC based algorithm is 0.37 s, manifesting that the MPC based algorithm can complete the reference-traced energy management instantaneously. The memory demand is also quite low, compared with the total memory of the simulation platform. The evaluation on communication delay of the MEC based framework, computational effort by IDP and MPC validates that the proposed optimal control strategy can be reasonably applied in real time.

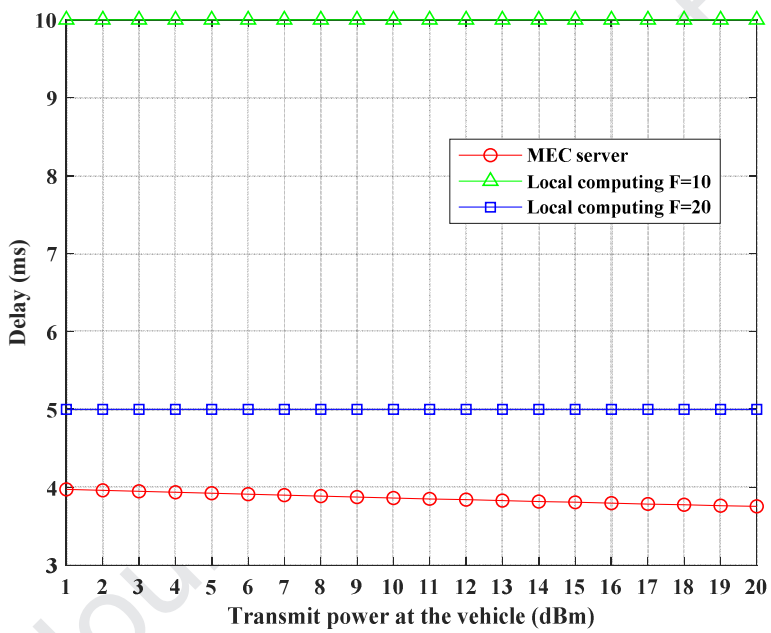


Fig. 18. Delay versus transmit power at the vehicle.

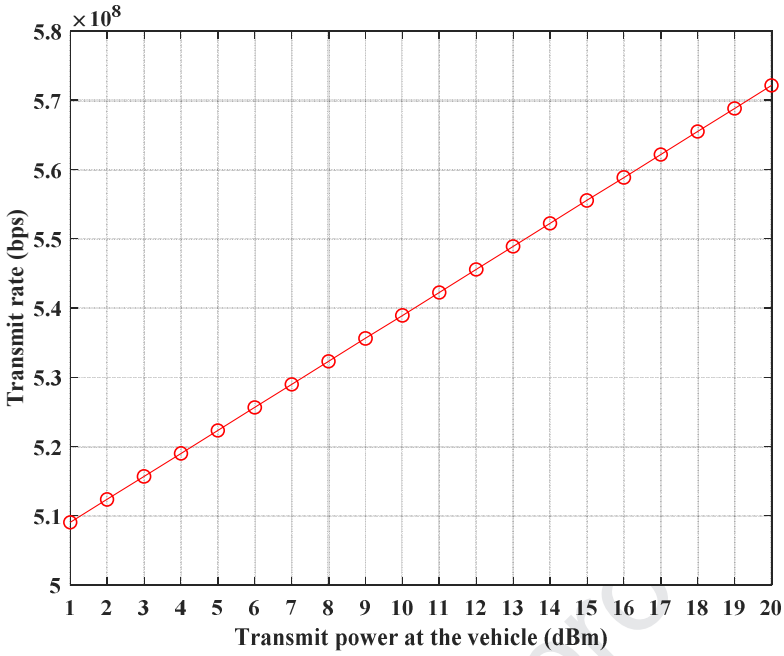


Fig. 19. Transmit rate versus transmit power at the vehicle.

Table 7 Comparison the computational effort by different strategies in energy utilization plan

Travel Route	Control Strategy	Route Segment	Segment CPU Calculation Time (s)	Total CPU Calculation Time (s)
1	DP	R1	-	7709.3937
		R2	-	
		R3	-	
	DP-Seg	R1	820.4321	2465.1271
		R2	823.9305	
		R3	820.7645	
	IDP-Seg	R1	97.6189	292.9214
		R2	96.1437	
		R3	99.1588	
2	DP	R1	-	7707.1495
		R2	-	
		R3	-	
	DP-Seg	R1	1106.2491	3315.5511
		R2	1103.4226	
		R3	1105.8794	
	IDP-Seg	R1	104.5268	311.0567
		R2	103.9876	
		R3	102.5432	

Table 8 Computational effort in energy utilization management

Method	Calculation time in each step	Memory usage
MPC	0.37s	97 Mb

Journal Pre-proof

V. CONCLUSION

This paper develops a cooperative control strategy based on a service-oriented hierarchical framework for plug-in hybrid electric vehicles. The energy flow between the engine and battery is optimally managed through a two-stage process by the proposed methods. The two-stage work, including the energy utilization plan and management, are performed in separate control units that are installed in roadside and vehicle, supporting the fast calculation. By iterative dynamic programming, the energy utilization in each route segment can be legitimately planned on the strength of estimated traffic information. The model predictive control based method can track the reference policies and fulfill the energy management. The simulation results manifest the advantage and feasibility of the raised strategy. The newly developed cooperative strategy presents one of distinctive solutions for plug-in hybrid electric vehicles, optimally managing power flow within powertrains and further exploiting energy-saving potential. Plug-in hybrid electric vehicles, as one representative of strong cleaner production, will contribute more to environment improvement and natural resources savings with the optimized control strategies, pushing the auto industry to move towards the age of sustainability.

In the future, more research will be conducted in the communication methods to improve the performance of cooperative control strategy. The mechanism underlines that the mobile edge computation needs to be carefully dealt with to determine the appropriate mobile edge computation unit number for each route segment with a certain length. Due to the errors raised in the model predictive control methods, the nonlinear model predictive control methods will be further investigated to achieve better performance. The proposed method will be applied to plug-in hybrid electric vehicles with different configurations, trying to enlarge the expandability. Moreover, the multi-vehicle energy collaborative optimization based on the raised hierarchical framework will be further investigated.

ACKNOWLEDGEMENT

This work was supported in part by the National Natural Science Foundation of China (No. 61763021 and No. 51775063), in part by the National Key R&D Program of China (No. 2018YFB0104900), and in part by the EU-funded Marie Skłodowska-Curie Individual Fellowships

Project under Grant 845102-HOEMEV-H2020-MSCA-IF-2018.

REFERENCE

[1] De Souza, Lidiane La Picirelli, et al. "Comparative environmental life cycle assessment of conventional vehicles with different fuel options, plug-in hybrid and electric vehicles for a sustainable transportation system in Brazil." Journal of cleaner production 203 (2018): 444-468.

[2] Wang, Chun, et al. "Comparison of decomposition levels for wavelet transform based energy management in a plug-in hybrid electric vehicle." Journal of cleaner production 210 (2019): 1085-1097.

[3] Shamshirband, Mehdi, Javad Salehi, and Farhad Samadi Gazijahani. "Decentralized trading of plug-in electric vehicle aggregation agents for optimal energy management of smart renewable penetrated microgrids with the aim of CO2 emission reduction." Journal of Cleaner Production 200 (2018): 622-640.

[4] Cusenza, Maria Anna, et al. "Energy and environmental assessment of a traction lithium-ion battery pack for plug-in hybrid electric vehicles." Journal of cleaner production 215 (2019): 634-649.

[5] J. Peng, H. He, and R. Xiong, "Rule based energy management strategy for a series–parallel plug-in hybrid electric bus optimized by dynamic programming," Applied Energy, vol. 185, pp. 1633-1643, 2017.

[6] M. F. M. Sabri, K. A. Danapalasingam, and M. F. Rahmat, "Improved Fuel Economy of Through-the-Road Hybrid Electric Vehicle with Fuzzy Logic-Based Energy Management Strategy," International Journal of Fuzzy Systems, vol. 20, no. 8, pp. 2677-2692, 2018.

[7] Z. Chen, R. Xiong, and J. Cao, "Particle swarm optimization-based optimal power management of plug-in hybrid electric vehicles considering uncertain driving conditions," Energy, vol. 96, pp. 197-208, 2016.

[8] Y. Zeng, "Parameter optimization of plug-in hybrid electric vehicle based on quantum genetic algorithm," Cluster Computing, pp. 1-9, 2018.

[9] W. Zhou, L. Yang, Y. Cai, and T. Ying, "Dynamic programming for New Energy Vehicles based on their work modes part I: Electric Vehicles and Hybrid Electric Vehicles," Journal of Power Sources, vol. 406, pp. 151-166, 2018.

[10] J. Liu, Y. Chen, J. Zhan, and F. Shang, "Heuristic Dynamic Programming-based On-line Energy Management Strategy for Plug-in Hybrid Electric Vehicles," IEEE Transactions on Vehicular Technology, 2019.

[11] X. Wu, X. Hu, X. Yin, L. Li, Z. Zeng, and V. Pickert, "Convex programming energy management and components sizing of a plug-in fuel cell urban logistics vehicle," Journal of Power Sources, vol. 423, pp. 358-366, 2019/05/31/ 2019.

[12] Bai, Y., He, H., Li, J., Li, S., Wang, Y. X., & Yang, Q.. Battery anti-aging control for a plug-in hybrid electric vehicle with a hierarchical optimization energy management strategy. Journal of Cleaner Production, 237, 117841. 2019

[13] Li, Yunwu, et al. "Hybrid energy storage system and energy distribution strategy for four-wheel independent-drive electric vehicles." Journal of Cleaner Production 220 (2019): 756-770.

[14] Yang, Yalian, et al. "Fuel economy optimization of power split hybrid vehicles: A rapid dynamic programming approach." Energy 166 (2019): 929-938. [15] A. Rezaei, J. B. Burl, and B. Zhou, "Estimation of the ECMS Equivalent Factor Bounds for Hybrid Electric Vehicles," IEEE Transactions on Control Systems and Technology, vol. 26, no. 6, pp. 2198-2205, 2018.

[16] S. Xie, X. Hu, Z. Xin, and L. Li, "Time-Efficient Stochastic Model Predictive Energy Management for a Plug-In Hybrid Electric Bus With an Adaptive Reference State-of-Charge Advisory," IEEE Transactions on Vehicular Technology, vol. 67, no. 7, pp. 5671-5682, 2018.

[17] B. Zhou, J. Burl, and A. Rezaei, "Hybrid electric vehicle battery aging estimation and economic analysis based on equivalent consumption minimization strategy," SAE Technical Paper0148-7191, 2017.

[18] Y. Huang, H. Wang, A. Khajepour, H. He, and J. Ji, "Model predictive control power management strategies for HEVs: A review," Journal of Power Sources, vol. 341, pp. 91-106, 2017/02/15/ 2017.

[19] Tian, Xiang, et al. "An adaptive ECMS with driving style recognition for energy optimization of parallel hybrid electric buses." Energy 189 (2019): 116151.

[20] Lei, Zhenzhen, et al. "An Adaptive Equivalent Consumption Minimization Strategy for Plug-in Hybrid Electric Vehicles Based on Traffic Information." Energy (2019): 116409.

[21] Guo, Qiuyi, et al. "Adaptive optimal control based on driving style recognition for plug-in hybrid electric vehicle." Energy 186 (2019): 115824.

[22] Montazeri-Gh, Morteza, and Mehdi Mahmoodi-K. "Optimized predictive energy management of plug-in hybrid electric vehicle based on traffic condition." Journal of cleaner production 139 (2016): 935-948.

[23] Z. Chen, L. Li, X. Hu, B. Yan, and C. Yang, "Temporal-Difference Learning-Based Stochastic Energy Management for Plug-in Hybrid Electric Buses," IEEE Transactions on Intelligent Transportation Systems, vol. 20, no. 6, pp. 2378-2388, 2019.

[24] C. Sun, F. Sun, and H. He, "Investigating adaptive-ECMS with velocity forecast ability for hybrid electric vehicles," Applied Energy, vol. 185, pp. 1644-1653, 2017.

[25] Li, Yang, and Xiaohong Jiao. "Real-time energy management for commute HEVs using modified A-ECMS with traffic information recognition." IET Intelligent Transport Systems 13.4 (2018): 729-737.

[26] Onori, Simona, and Laura Tribioli. "Adaptive Pontryagin's Minimum Principle supervisory controller design for the plug-in hybrid GM Chevrolet Volt." Applied Energy 147 (2015): 224-234.

[27] D. Jocic, V. Cirovic, and D. Aleksendric, "Identification and Recognition of Vehicle Environment Using Artificial Neural Networks," in Experimental and Numerical Investigations in Materials Science and Engineering: Springer, 2018, pp. 208-219.

Journal Pre-proof

[28] J. Shin and M. Sunwoo, "Vehicle Speed Prediction Using a Markov Chain With Speed Constraints," IEEE Transactions on Intelligent Transportation Systems, pp. 1-11, 2018.

[29] C. Sun, X. Hu, S. J. Moura, and F. Sun, "Velocity Predictors for Predictive Energy Management in Hybrid Electric Vehicles," IEEE Transactions on Control Systems and Technology, vol. 23, no. 3, pp. 1197-1204, 2015.[30] F. Zhang, X. Hu, R. Langari, and D. Cao, "Energy management strategies of connected HEVs and PHEVs: Recent progress and outlook," Progress in Energy and Combustion Science, vol. 73, pp. 235-256, 2019.

[31] H. Lim and W. Su, "Hierarchical Energy Management for Power-Split Plug-In HEVs Using Distance-Based Optimized Speed and SOC Profiles," IEEE Transactions on Vehicular Technology, vol. 67, no. 10, pp. 9312-9323, 2018.

[32] H. Lim, C. C. Mi, and W. Su, "A Distance-Based Two-Stage Ecological Driving System Using an Estimation of Distribution Algorithm and Model Predictive Control," IEEE Transactions on Vehicular Technology, vol. 66, no. 8, pp. 6663-6675, 2017.

[33] Y. Wu, H. Tan, J. Peng, H. Zhang, and H. He, "Deep reinforcement learning of energy management with continuous control strategy and traffic information for a series-parallel plug-in hybrid electric bus," Applied Energy, vol. 247, pp. 454-466, 2019/08/01/ 2019.

[34] C. Zhu, F. Lu, H. Zhang, J. Sun, and C. C. Mi, "A Real-Time Battery Thermal Management Strategy for Connected and Automated Hybrid Electric Vehicles (CAHEVs) Based on Iterative Dynamic Programming," IEEE Transactions on Vehicular Technology, vol. 67, no. 9, pp. 8077-8084, 2018.

[35] Y. Cao et al., "Toward Efficient, Scalable, and Coordinated On-the-Move EV Charging Management," IEEE Wireless Communications, vol. 24, no. 2, pp. 66-73, 2017.

[36] S. Biswas, R. Tatchikou and F. Dion, "Vehicle-to-vehicle wireless communication protocols for enhancing highway traffic safety," IEEE Communications Magazine, vol. 44, no. 1, pp. 74-82, Jan. 2006.

[37] Zhu, Chong, et al. "A real-time battery thermal management strategy for connected and automated hybrid electric vehicles (CAHEVs) based on iterative dynamic programming." IEEE Transactions on Vehicular Technology 67.9 (2018): 8077-8084.

[38] V. Doan, H. Fujimoto, T. Koseki, T. Yasuda, H. Kishi, and T. Fujita, "Iterative Dynamic Programming for Optimal Control Problem with Isoperimetric Constraint and Its Application to Optimal Eco-driving Control of Electric Vehicle," IEEJ journal of industry applications, vol. 7, no. 1, pp. 80-92, 2018.

[39] Y. Zhang et al., "Optimal energy management strategy for parallel plug-in hybrid electric vehicle based on driving behavior analysis and real time traffic information prediction," Mechatronics, vol. 46, pp. 177-192, 2017.

[40] D. Ariens, B. Houska, H. Ferreau, and F. Logist, "Acado for Matlab user's manual," Optimization in Engineering Center (OPTEC), vol. 1, 2010.

[41] D. Ariens, B. Houska, H. Ferreau, and F. Logist, "Acado: Toolkit for automatic control and dynamic optimization," Optimization in Engineering Center (OPTEC), vol. 1, 2010.

[42] Hao, Wanming, et al. "Green communication for NOMA-based CRAN." IEEE Internet of things journal 6.1 (2018): 666-678.

Journal Pre-proof

Journal Pre-proof

Cooperative Control Strategy for Plug-in Hybrid Electric Vehicles Based on a Hierarchical Framework with Fast Calculation

Highlights

- A fast calculation control strategy is raised for plug-in hybrid electric vehicles
- The hierarchical framework is built to uphold the implementation of strategy
- Iterative dynamic programming attains fast global optimization
- Model predictive control completes global optimal control policy tracking

Journal Pre-proof

Yuanjian Zhang: Conceptualization, Methodology, Writing-Original draft preparation, Writing-Reviewing and Editing. **Chong Guo**: Writing-Original draft preparation. **Guang Li**: Methodology, Writing. **Yonggang Liu**: Investigation, Supervision. **Zheng Chen**: Supervision, Writing-Original draft preparation, Writing-Reviewing and Editing.

Journal Pre-proof

Journal Pre-proof

Declaration of interests

☒ The authors declare that they have no known competing financial interests or personal relationships that could have appeared to influence the work reported in this paper.

☐The authors declare the following financial interests/personal relationships which may be considered as potential competing interests:

Journal Pre-proof